Many-Body Coherent Destruction of Tunneling

Jiangbin Gong,[1,2,*] Luis Morales-Molina,[1,3] and Peter Hänggi[1,4]

[1]*Department of Physics and Center for Computational Science and Engineering, National University of Singapore, Singapore 117542, Singapore*

[2]*NUS Graduate School for Integrative Sciences and Engineering, Singapore 117597, Singapore*

[3]*Facultad de Física, Pontificia Universidad Católica de Chile, Santiago 22, Chile*

[4]*Theoretische Physik I, Institut für Physik, Universität Augsburg, D-86135 Augsburg, Germany*

(Received 26 April 2009; published 23 September 2009)

A new route to coherent destruction of tunneling is established by considering a monochromatic fast modulation of the self-interaction strength of a many-boson system. The modulation can be tuned such that only an arbitrarily, *a priori* prescribed number of particles are allowed to tunnel. The associated tunneling dynamics is sensitive to the odd or even nature of the number of bosons.

DOI: 10.1103/PhysRevLett.103.133002 PACS numbers: 32.80.Qk, 03.65.Xp, 33.80.Be

The phenomenon of coherent destruction of tunneling (CDT) [1,2] by a driving field has been one seminal result in studies of quantum dynamics control. Direct observation of CDT was recently achieved in several experiments [3,4], one of which [4] involving noninteracting cold atoms in a double-well potential. CDT in interacting many-body systems has also attracted considerable interest, with previous work focusing on driving fields on resonance with the interaction energy [5,6]. The Mott-superfluid transition in ultracold systems via a mechanism similar to single-particle CDT has also been observed experimentally [7].

Traditionally, the driving field in CDT studies is to directly modulate the bare single-particle levels of an undriven system. For example, in a two-level theory of CDT, the driving field is to modulate the energy difference between two bare levels. By contrast, in this work we expose a new route to CDT by taking advantage of the particle-particle interaction in a many-body system. Specifically, we consider the CDT in a two-mode Bose-Hubbard model that describes a two-mode Bose-Einstein condensate (BEC). We show, both analytically and computationally, that a monochromatic off-resonance driving of the self-interaction strength of the BEC can induce different types of CDT without a direct modulation of the mode-energy bias. Interestingly, this makes it possible to precisely control, at least in principle, the number of bosons allowed to tunnel. Another remarkable prediction is the sensitivity of the full-quantum dynamics to the even or odd nature of the number of bosons. Note that in other contexts such as matter-wave solitons, intriguing effects of a periodic modulation of the self-interaction strength of a BEC (the so-called ''Feshbach-resonance management'') have been discovered [8], but on the mean-field level only.

Consider then the following Bose-Hubbard Hamiltonian for a two-mode BEC:

$$H = v\hbar(a_l^\dagger a_r + a_r^\dagger a_l)/2 + g(t)\hbar(a_l^\dagger a_l - a_r^\dagger a_r)^2/4, \quad (1)$$

where r and l are mode indices, a_k and $a_k^\dagger$ ($k = r, l$) are the bosonic annihilation and creation operators, v describes the constant tunneling rate between the two modes, and $g(t)$ is the interaction strength between same-mode bosons. We use the unit of v to appropriately scale all the parameters such that v, $g(t)$, and t all become dimensionless variables. The total number of bosons $N = a_l^\dagger a_l + a_r^\dagger a_r$ is a conserved quantity and the dimension of the Hilbert space is $N + 1$. Using the Schwinger representation of angular momentum operators, namely, $J_x = (a_l^\dagger a_r + a_r^\dagger a_l)/2$, $J_y = (a_r^\dagger a_l - a_l^\dagger a_r)/(2i)$, and $J_z = (a_l^\dagger a_l - a_r^\dagger a_r)/2$, Eq. (1) reduces to

$$H(t) = v\hbar J_x + g(t)\hbar J_z^2. \quad (2)$$

The Hilbert space is expanded by the eigenstates of J_z, denoted $|m\rangle$, with $J_z|m\rangle = m|m\rangle$. The mode population difference is given by the expectation value of $2J_z$. For later use, we also define $J_+ \equiv J_x + iJ_y$. Note that there is no energy bias between the two modes and that the time dependence of the Hamiltonian arises from $g(t)$, which is assumed to be [8]

$$g(t) = g_0 + g_1 \cos(\omega t). \quad (3)$$

Under appropriate conditions $H(t)$ describes a BEC distributed in the two wells of a double-well potential [4], in the ground band and the first-excited band associated with an accelerating optical lattice [9], or in two hyperfine levels. For convenience, below we focus on the first context, which can be best realized by optical superlattices [10]. Hence $r(l)$ denotes the right (left) well. Our central idea is to use an off-resonance oscillation in $g(t)$ to switch off the tunneling between the left and right wells.

The Floquet operator associated with $H(t)$ is given by $\hat{F} \equiv \mathcal{T}\{\exp[-i\int_0^{2\pi/\omega} H(t')/\hbar dt']\}$, where $\mathcal{T}$ is the time-ordering operator. Its eigenstates are the Floquet states, with eigenvalues $\exp(-i\epsilon 2\pi/\hbar\omega)$, where ϵ is the quasienergy. Because $H(t)$ apparently possesses a parity symmetry, namely, it is invariant upon an exchange of the

indices l and r, the Floquet states can be chosen as either positive-parity or negative-parity states. If two opposite-parity Floquet states cross or touch, then similar to the single-particle CDT mechanism, their superposition, which is still a Floquet state, breaks the left-right symmetry and hence CDT occurs [11].

Figure 1 depicts that the degeneracy between opposite-parity states can easily occur, thus suggesting that CDT is possible via solely a monochromatic modulation in the self-interaction strength. Next, we examine some detailed features presented in Fig. 1, for $g_0 = 0$, $N = 10$, and $\upsilon = 1$ as an example. In Fig. 1(a), $\omega = 40 \gg \upsilon = 1$, and three values of g_1/ω for which level degeneracies occur are explicitly marked by vertical dashed lines. At point I, the level crossing involves two positive-parity states and one negative-parity state. At point II, two pairs of opposite-parity states become degenerate simultaneously. At point III, three states in the middle of the Floquet spectrum cross, and two additional pairs of opposite-parity Floquet states also touch each other. Similar spectral patterns can be found in other regimes of g_1/ω. In Fig. 1(b), $\omega = 2\pi$ is quite comparable to $\upsilon = 1$. In this intermediate-frequency case, the spectral patterns become more complicated. Nevertheless, as indicated by those vertical dashed lines in Fig. 1(b), when g_1 increases, the spectral pattern in Fig. 1(b) becomes analogous to those seen in Fig. 1(a).

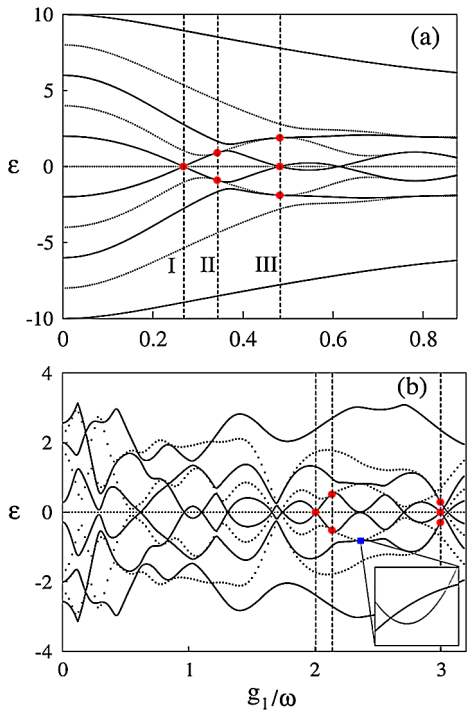

FIG. 1 (color online). Quasienergy spectrum versus g_1/ω. Vertical dashed lines indicate the location (i.e., $g_1/\omega \sim 0.267$, 0.344, and 0.481) of level degeneracies. Dotted (solid) lines are for states with negative (positive) parity. $N = 10$, $g_0 = 0$, and $\upsilon = 1$. In (a), $\omega = 40$ and in (b), $\omega = 2\pi$. Spectral details around the square are shown in the inset in (b), with two-level-crossings. Here and in other figures all variables are dimensionless.

We develop below a theory for the Floquet spectrum in the high-frequency regime, with its validity condition elaborated later. In that regime, the full Floquet theory can be expanded to the first order of $1/\omega$ [2] and a static effective Hamiltonian H_{eff} for the driven quantum dynamics can be obtained by averaging out the driving-field effects [12]. Explicitly,

$$H_{\text{eff}} = \frac{\omega}{2\pi}\int_0^{2\pi/\omega} e^{[iA(t)J_z^2]}(g_0\hbar J_z^2 + \upsilon\hbar J_x)e^{[-iA(t)J_z^2]}dt, \tag{4}$$

where $A(t) = \int_0^t g_1\cos(\omega t)dt = (g_1/\omega)\sin(\omega t)$. Using the identity in the SU(2) algebra, i.e., $e^{iA(t)J_z^2}J_x e^{-iA(t)J_z^2} = (J_+/2)e^{iA(t)(2J_z+1)} + \text{c.c.}$, where c.c. means complex conjugate of the preceding term, and substituting this into Eq. (4) to perform the integral, we obtain the effective Hamiltonian,

$$H_{\text{eff}} = g_0\hbar J_z^2 + (\upsilon\hbar J_+/2)\mathcal{J}_0[g_1(2J_z + 1)/\omega] + \text{c.c.}, \tag{5}$$

where $\mathcal{J}_0(x)$ is the ordinary Bessel function of order zero. Equation (5) indicates that the net effect of a fast modulation in $g(t)$ is the rescaling factor $\mathcal{J}_0[g_1(2J_z + 1)/\omega]$, which depends on J_z, i.e., the population difference between the two wells. Further, a nonzero g_0 leads to the $g_0\hbar J_z^2$ term in H_{eff}. It is well known that this term can induce population localization via a self-trapping mechanism. To isolate population localization due to possible CDT phenomena from that due to self-trapping, we will not consider cases with nonzero g_0 until much later.

In the eigenrepresentation of J_z, H_{eff} is a tridiagonal matrix. Further, if $\langle m-1|H_{\text{eff}}|m\rangle = 0$, then $\langle m|H_{\text{eff}}|m-1\rangle = 0$, and we must also have $\langle 1-m|H_{\text{eff}}|-m\rangle = \langle -m|H_{\text{eff}}|1-m\rangle = 0$ due to symmetry consideration. These four zero matrix elements divide the tridiagonal matrix of H_{eff} into three uncoupled subspaces, i.e.,

$$H_{\text{eff}} = \begin{bmatrix} h_l & 0 & 0 \\ 0 & h_i & 0 \\ 0 & 0 & h_r \end{bmatrix}, \tag{6}$$

where h_l represents a submatrix of H_{eff} in the subspace spanned by states $|N/2\rangle, |N/2-1\rangle, \ldots, |m\rangle$ (assuming $m > 0$), h_r represents a submatrix of H_{eff} in the subspace spanned by states $|-N/2\rangle, |-N/2+1\rangle, \ldots, |-m\rangle$, and h_i represents the third block matrix involving other remaining basis states. Therefore, if $\langle m-1|H_{\text{eff}}|m\rangle = 0$, then (i) the transition between $|m\rangle$ ($|-m\rangle$) and all other basis states $|m'\rangle$ ($|-m'\rangle$) with $m' < m$ will not occur, (ii) the Floquet states must display degeneracy because h_r is identical with h_l due to the parity symmetry of $H(t)$, and (iii) the dimension of h_r or h_l, namely, $(N/2 - m + 1)$, also gives the expected number of degenerate pairs.

Suppose there are $N - i$ (i) particles in the left (right) well. Without loss of generality, we assume $i < N/2$. The associated quantum state is given by $|m\rangle = |N/2 - i\rangle$. Using Eq. (5), one finds that the condition $\langle m - 1|H_{\rm eff}|m\rangle = 0$ is equivalent to

$$\mathcal{J}_0\{g_1[N - (2i + 1)]/\omega\} = 0. \quad (7)$$

As such, if $g_1[N - (2i + 1)]/\omega$ is tuned to become one root of $\mathcal{J}_0(x)$, then the tunneling of one more particle from the left well to the right well (hence $m \to m - 1$) becomes prohibited if the left well has already released i particles to the right well.

We now compare the theoretical result of Eq. (7) with our computationally precise results in Fig. 1. For the cases in Fig. 1(a), theoretically the spectral degeneracy is expected to occur when $g_1[10 - (2i + 1)]/\omega$ becomes a root of $\mathcal{J}_0(x)$. In particular, for the first root of $\mathcal{J}_0(x)$ at $x \sim 2.405$ and for $i = 0$, 1, 2, the predicted degeneracy is at $g_1/\omega \approx 0.267$, 0.344, and 0.481, with the pair number of level degeneracies in each case given by the dimension of h_r, i.e., $i + 1$. This is in perfect agreement with the three marked degeneracy points shown in Fig. 1(a). It is now also possible to explain why the level crossings in the middle of the spectrum in Fig. 1(a) can involve three states. This is because (i) if N is even and $g_0 = 0$, $H_{\rm eff}$ always has a zero eigenvalue due to its tridiagonal structure, and (ii) when the dimension of h_r and h_l is odd, they can present two additional zero eigenvalues. Interestingly, for sufficiently large g_1, such agreement between theory and numerics may persist for the intermediate-frequency case in Fig. 1(b). For example, the degeneracies marked by the three vertical lines in Fig. 1(b) occur at $g_1/\omega \sim 2.007$, 2.133, and 2.986. These values, when multiplied by $[N - (2i + 1)]$ for $i = 0$, 1, 2, respectively, are the 6th or 5th root of $\mathcal{J}_0(x)$. Note, however, that the subtle crossing behavior depicted in the inset of Fig. 1(b) is beyond our theory.

With a normalized population imbalance $\langle S\rangle \equiv 2\langle J_z\rangle/N$, Fig. 2(a) shows the numerically exact population dynamics associated with the three marked points in Fig. 1(a). The initial state is that all particles are in the left well. In the first case for $g_1/\omega \sim 0.267$, $\langle S\rangle$ is seen to stay at almost unity and hence in essence the tunneling between the two wells is completely suppressed. In the second case for $g_1/\omega \sim 0.344$, our theory predicts that the tunneling suppression occurs only when $\langle S\rangle$ becomes 0.8. As seen in Fig. 2(a), $\langle S\rangle$ indeed oscillates between 0.8 and 1.0. Similarly, in the third case, $\langle S\rangle$ oscillates between 1.0 and ~0.6, confirming our theory that the tunneling stops if two particles are already released to the right well. Excellent agreement is obtained at other level degeneracy points. These features signify one key aspect of our many-body CDT: It depends sensitively on the number of particles that have already tunneled. With the same initial condition, in Fig. 2(b) we also show the three intermediate-frequency cases marked earlier by the vertical lines in Fig. 1(b). The associated population dynamics still agrees

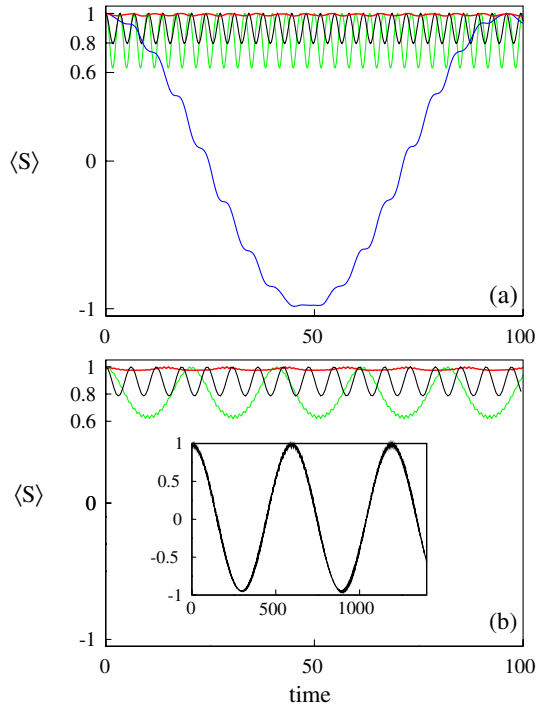

FIG. 2 (color online). (a) Time dependence of $\langle S\rangle$ for $g_0 = 0$ and $N = 10$, with $\omega = 40$ in (a) and $\omega = 2\pi$ in (b). From top to bottom, values of g_1/ω are associated with the three vertical lines (from left to right) in Fig. 1(a) for panel (a) and in Fig. 1(b) for panel (b). For comparison, a case with $g_1/\omega = 10.5/40 = 0.2625$ is also shown in (a). The inset of (b) is for the first level crossing shown in the inset of Fig. 1(b).

with our theory. Because the predicted CDT points are independent of the actual tunneling rate υ, we found that even if an oscillation in υ is considered [which can be induced by the modulation in $g(t)$], analogous results can be obtained. For the case shown in the inset of Fig. 1(b), which is beyond our high-frequency theory, almost complete population delocalization is observed in the inset of Fig. 2(b).

Figures 3(a)–3(c) schematically illustrate the three representative CDT cases studied in Figs. 1(a) and 2(a). In Fig. 3(a), no particle is allowed to tunnel, and in Figs. 3(b) and 3(c), one or two particles have tunneled and then CDT occurs. Consistent with this picture, Fig. 3(d) depicts the numerically time-averaged $\langle S\rangle$, denoted $\langle\langle S\rangle\rangle$, as a function of g_1/ω, for $N = 10$ and $\omega = 40$. It is seen that as g_1/ω is scanned at a rather low resolution, the value of $\langle\langle S\rangle\rangle$ is either zero or close to "magic" nonzero numbers (~1.0, ~0.9, and ~0.8, ...). Figures 3(a)–3(c) also provoke us to reinterpret our theoretical finding. In particular, for $g_0 = 0$, the energy difference between the two configurations in Figs. 3(a) and 3(b) [Figs. 3(b) and 3(c)] is $g_1\hbar\cos(\omega t) \times [N - (2i + 1)]$ with $i = 0$ ($i = 1$). As such, even though there is no direct modulation of the energy bias between the two wells, the oscillation in $g(t)$ still causes a modulation of the *effective* bias between different configurations. With this interpretation, we are able to rederive Eq. (7)

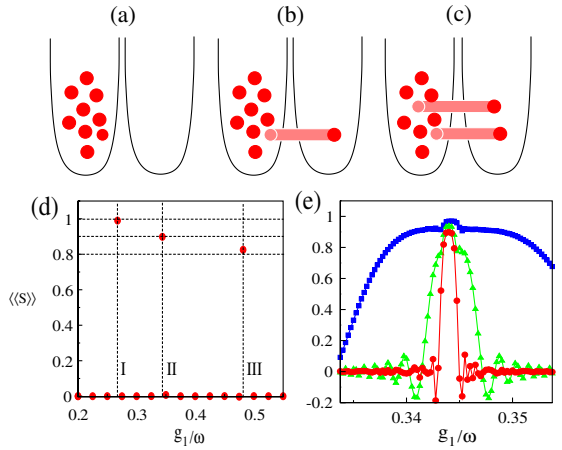

FIG. 3 (color online). (a)–(c) Schematic picture of particle-number-dependent CDT. In case (a), no particle tunnels, and in cases (b) and (c), only one or two particles tunnel and then CDT occurs. (d) Long-time average of $\langle\langle S\rangle\rangle$ versus g_1/ω for $\omega = 40$ and $g_0 = 0$, with g_1/ω scanned at a rather low resolution. (e) Same as in (d), but with g_1/ω scanned in small steps around the regime of 0.343, with $g_0/\omega = 1/144$ (■), $g_0/\omega = 1/288$ (▲), and $g_0 = 0$ (●). The total time used for averaging is 20 000 in dimensionless units.

by analogy to standard single-particle CDT theory. This analogy also makes clear that the precise condition for our high-frequency approximation should be $\tilde{v} \ll \max(\omega, \sqrt{\epsilon\omega})$ [2], where $\tilde{v} \equiv v\sqrt{(N-i)(i+1)}$ is the coupling strength between states $|N/2-i\rangle$ and $|N/2-i-1\rangle$, and $\epsilon \equiv |g_1[N-(2i+1)]|$ is the amplitude of the effective bias. For $i \ll N$, this condition becomes $v \ll \max(\frac{\omega}{\sqrt{N}}, \sqrt{g_1\omega})$. This well explains our early observation from Fig. 1(b) that as g_1 increases, the spectral pattern in intermediate-frequency cases starts to resemble those in Fig. 1(a) and becomes more perspicuous with our theory.

Let us now turn to cases with nonzero g_0. If the system is close to a CDT point, $\mathcal{J}_0[g_1(2J_z+1)/\omega]$ is small, the g_0 term in H_{eff} will dominate, and hence the associated self-trapping effect may induce a strong population imbalance on a very long-time scale. Taking one small window of g_1/ω in Fig. 3(d) as an example, we compare $g_0 \neq 0$ with $g_0 = 0$ cases in Fig. 3(e). Clearly, as g_0 increases, the width of the $\langle\langle S\rangle\rangle$ profile in Fig. 3(e) increases significantly. This interplay between self-trapping and CDT is analogous to that in a two-mode optical waveguide system where the mode bias is periodically modulated [13]. The peak value of $\langle\langle S\rangle\rangle$ is also seen to change with g_0. We conclude that on one hand, a small nonzero g_0 is beneficial to experiments because it reduces the sensitivity of $\langle\langle S\rangle\rangle$ to the exact values of g_1/ω; on the other hand, however, the predicted particle-number-dependent CDT effect may be buried by self-trapping if g_0 is too large.

Our findings have potential applications in probing and exploring genuine quantum coherence in BEC. In particular, the dynamics under a preestablished CDT condition may be dramatically changed upon adding bosons to the system. As an example, we consider the CDT point I in Fig. 1(a), where $\mathcal{J}_0[g_1(N-1)/\omega] = 0$ for $N = 10$. If we let $N \to N+2$ by adding two particles to the left well, then because we still have $\mathcal{J}_0\{g_1[(N+2)-3]/\omega\} = 0$, Eq. (7) suggests that the CDT will be reestablished after one particle is tunneled to the right well. However, if we let $N \to N+1$ by adding only one particle to the left well, then because $(N-1)$ cannot be written as $(N+1)-(2i+1)$ for any i, $\mathcal{J}_0\{g_1[(N+1)-(2i+1)]/\omega\}$ is in general nonzero for fixed g_1/ω, and as a result, all of the particles start to tunnel back and forth between the two wells. The minor difference between adding an even and adding an odd number of bosons is thus greatly amplified by CDT, a prediction also confirmed by our numerical experiments. Similar behavior is obtained if more particles are added to the system. This odd-even sensitivity to the particle number is absent in any mean-field theory of a BEC, providing a possible means for accurate counting or efficient filtering of the number of bosons. Certainly, as implied by the results in Fig. 3(e), this is possible only if g_0 is sufficiently small such that the $\langle\langle S\rangle\rangle$ profiles associated with different particle numbers do not overlap.

This work is supported by WBS Grants No. R-144-050-193-101/133 and No. R-144-000-195-101 (J. G.), and by German Excellence Initiative via the Nanosystems Initiative Munich (NIM) (P. H.).

*phygj@nus.edu.sg

[1] F. Grossmann *et al.*, Phys. Rev. Lett. **67**, 516 (1991); F. Grossmann and P. Hänggi, Europhys. Lett. **18**, 571 (1992).
[2] M. Grifoni and P. Hänggi, Phys. Rep. **304**, 229 (1998).
[3] G. Della Valle *et al.*, Phys. Rev. Lett. **98**, 263601 (2007); H. Lignier *et al.*, Phys. Rev. Lett. **99**, 220403 (2007).
[4] E. Kierig *et al.*, Phys. Rev. Lett. **100**, 190405 (2008).
[5] C. E. Creffield and T. S. Monteiro, Phys. Rev. Lett. **96**, 210403 (2006); C. E. Creffield, Phys. Rev. A **75**, 031607 (2007).
[6] A. Eckardt and M. Holthaus, Phys. Rev. Lett. **101**, 245302 (2008).
[7] A. Zenesini *et al.*, Phys. Rev. Lett. **102**, 100403 (2009); A. Eckardt *et al.*, Phys. Rev. A **79**, 013611 (2009).
[8] P. G. Kevrekidis *et al.*, Phys. Rev. Lett. **90**, 230401 (2003); F. Kh. Abdullaev *et al.*, Phys. Rev. A **68**, 053606 (2003); H. Saito and M. Ueda, Phys. Rev. Lett. **90**, 040403 (2003).
[9] Q. Zhang, P. Hänggi, and J. B. Gong, Phys. Rev. A **77**, 053607 (2008), and references therein.
[10] S. Fölling *et al.*, Nature (London) **448**, 1029 (2007); M. Anderlini *et al.*, Nature (London) **448**, 452 (2007).
[11] This is already exploited in a delta-kicked system; see M. P. Strzys, E. M. Graefe, and H. J. Korsch, New J. Phys. **10**, 013024 (2008).
[12] S. Kohler, J. Lehmann, and P. Hänggi, Phys. Rep. **406**, 379 (2005); see pp. 401–402.
[13] X. Luo, Q. Xie, and B. Wu, Phys. Rev. A **76**, 051802 (2007).